

VARIABLE EXTRUSION WIDTH FOR INTERLOCKING FEATURES IN FUSED FILAMENT FABRICATION 3D PRINTING

Osama Habbal¹, Dr. Georges Ayoub², Dr. Christopher Pannier¹

¹Department of Mechanical Engineering and ²Department of Industrial and Manufacturing Systems Engineering, University of Michigan-Dearborn, Dearborn, MI, USA

Abstract

Following from developments in continuously variable extrusion width in fused filament fabrication additive manufacturing, this work explores the combination of in-plane bead width variation with bead trajectory variation as a technique to improve in-plane strength in polymer material extrusion additive manufacturing. Sinusoidal in-plane waveforms are used for the extruder trajectory instead of maintaining a straight line. The varied bead width, in conjunction with the non-straight bead trajectory, reduces anisotropy of strength within the layer. The findings apply to fully dense infill of single layers, commonly called horizontal perimeters in common slicing/toolpath planning computer programs. Experimental tensile testing results show a 48.6% reduction in anisotropy of tensile strength driven by 43% and 29% increases in the ultimate tensile strength in the 0° and 45° orientations, respectively. However, this comes at the cost of 99.6% reduction in toughness in the 90° orientation. We also present the principal concept behind the machine code generating script, that allows for the increase and decrease of the extruded bead width continuously along the extruded bead.

Introduction

Fused filament fabrication (FFF) is an additive manufacturing method that uses a polymer filament as a building material to produce near net shape objects with great design freedom, but significantly less strength than molded or milled parts of the same material (Popescu et al., 2018). This filament is heated and liquefied in the extruder and then extruded into beads of uniform height and width. Generally, multiple beads of uniform height (necessarily deposited at the same vertical coordinate) create a layer. The collection of multiple 2D layers in the Z-axis direction creates the overall 3D object, as shown in Figure 1.

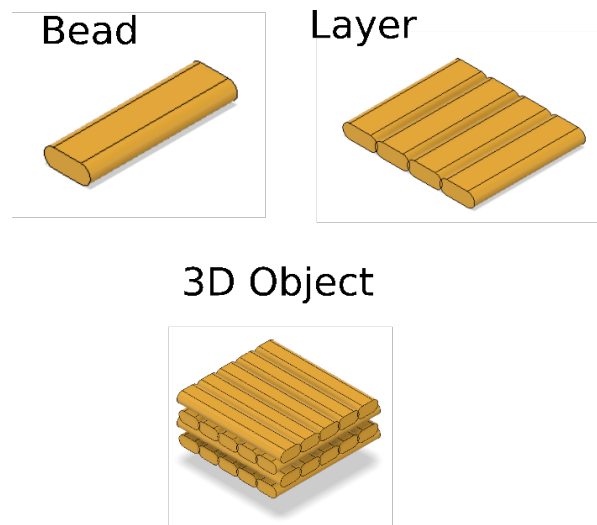


Figure 1 The building blocks of FFF 3D printed objects: beads and layers

Part strength is driven by bead interfaces. In the bead laying strategy of FFF, the bond that forms between the beads is less strong than the bulk strength of the thermoplastic polymer, because the bead adjacent to the current bead undergoing deposition has cooled. The problem is exacerbated for subsequent layers because the bead beneath the current layer is even cooler (Singh, Singh, Prakash & Ramakrishna, 2020). If mechanical loading occurs in-between the layers of the object (loading in the vertical direction), mechanical failure will occur between the layers, as the bond between the layers is weaker than the material within the layer. Similarly, within a single layer, the mechanical strength is lower across the bead-to-bead interface than in the direction parallel to the beads. Therefore, the basic fault is not solely due to the interlayer adhesion, rather, it is a manifestation of the basic lay-up method that FFF uses. To overcome the anisotropy within each layer and the inherent weakness due to the bead lay-up process, 3D printing slicer (toolpath generation) software applications stagger the in-plane angles from layer to layer to achieve a higher strength within the X-Y direction of the printed object. However, the staggered angles effectively lower the object's X-Y strength from its theoretical maximum since only a subset of the layers within the object have extruded beads parallel to the loading direction. Therefore, any attempt to increase the strength of 3D printed parts must target the core of the problem: the bead lay-up method.

The root cause for the weak bond between the extruded beads can be extrapolated from the way that each individual bead joins with the bead adjacent to it. Instead of an interface that covers the whole thickness of the bead, the two beads join in an interface that is shorter than the bead height. This reduced cross-sectional area concentrates mechanical stress, as stress is load force divided by cross-sectional area, thereby reducing the load force that the object can handle. A schematic rendering of a bead interface is shown in Figure 2.

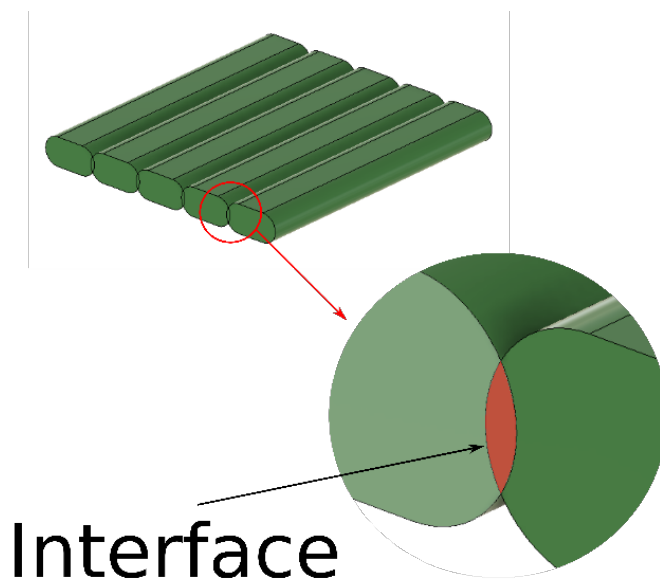


Figure 2 Close up view of the small interface bond between each individual extruded bead compared to the bead height

One potential solution to make up for the small interface area between beads is to select a tessellating bead laying pattern for the layer that has a longer interface length; straight lines can be replaced with other trajectories. A curved or otherwise non-linear pattern for the beads in the X-Y plane will be longer than a line since a line provides the shortest distance between two

points. As an example of a possible tessellating trajectory to provide increased bead interface length, a sine waveform pattern is shown in Figure 3. In this paper, we introduce a method for increasing the value of the in-layer strength of 3D printed objects with the use of an interlocking sine waveform extrusion pattern. The paper is organized as follows: background on relevant literature and mechanical testing standards, methods for printing and testing, results from tensile testing, and then conclusions and future directions.

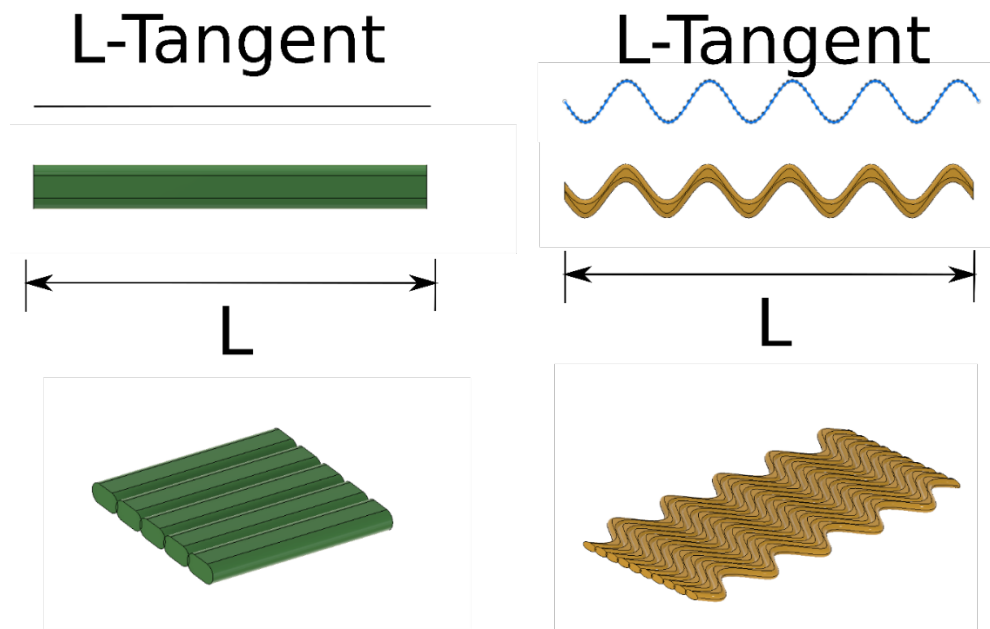


Figure 3 Interface length of a straight line vs. a sine waveform to span length L , with tangent line (“L-Tangent”) plotted above, indicating longer arclength of the sine waveform

Background

Strength at different orientations can vary widely in 3D printed objects; this topic was explored by Yao et al. for various X-Z loading directions (2019). The X-Z orientations of the tensile testing samples of that work are shown in Figure 4A. Their results show a large variation in strength depending on printed orientation and load direction. When pulling perpendicular to the interface between the extruded lines (the 0° X-Z orientation) the strength is 52% less than when pulling parallel to the beads (the 90° X-Z orientation).

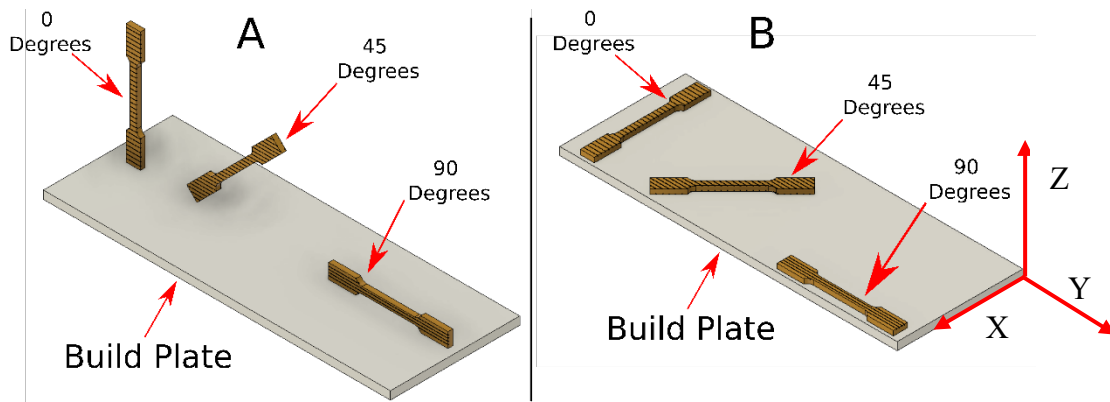


Figure 4 (A) 3D printed tensile test specimen X-Z orientations of Yao et al. (2019)
 (B) Orientations in the Methods section of the present paper are in-plane (X-Y).

Motivated by the problem of the tensile strength penalty of FFF compared to other manufacturing methods, Moetazedian et al. (2021) explores continuously varying the extruded bead width along a single extrusion line in FFF and calls this technique CONtinuously Varied EXtrusion (CONVEX). That work achieves reduced size and quantity of voids and defects in FFF parts by using extruded beads that increase or decrease in width along their length. These bead laying patterns, which the authors call “streamlined slicing”, fill 2-D space much like the streamlines in an expanding or converging laminar fluid flow. The authors create process maps between the inputs of speed, acceleration, extrusion rates and retractions and the output: the extruded bead width, but do not assess the tensile strength gains of CONVEX.

In order to conduct tensile testing of FFF parts, test samples with a dog bone shape are usually required. Direct printing of such samples can yield samples with variable mechanical properties (Cole et al., 2020). A method for producing uniform FFF samples by extraction from a sheet was introduced by Cole et al. (2020). The samples are produced by printing a large sheet of material of the desired number of layers, and then using a wet saw to extract samples of a given width and length as rectangular test specimens. Care is taken to extract the samples away from the edges of the sheet, so that stress concentration points are avoided.

Printing of sinusoids was previously introduced by Khurana et al. (2017), under the name of “Active Z-Printing”. That work explores the impact of sinusoidal layers on the flexural strength, but not ultimate tensile strength, of FFF parts. Bread slicer, an experimental slicing software, was used to create out-of-plane sinusoidal tool paths for each layer, for both perimeters and infill. The results show an increase in the flexural strength of the objects when using sinusoidal waveforms. This points to an opportunity to improve tensile strength using in-plane sine wave extrusion trajectories.

Methods

The bead waveform is created by initially plotting a sine wave and offsetting a copy of it in the Y direction by the desired extruded bead width. The resulting area in-between the two sine waves is the basic building block of the full pattern. This process is shown in Figure 5.

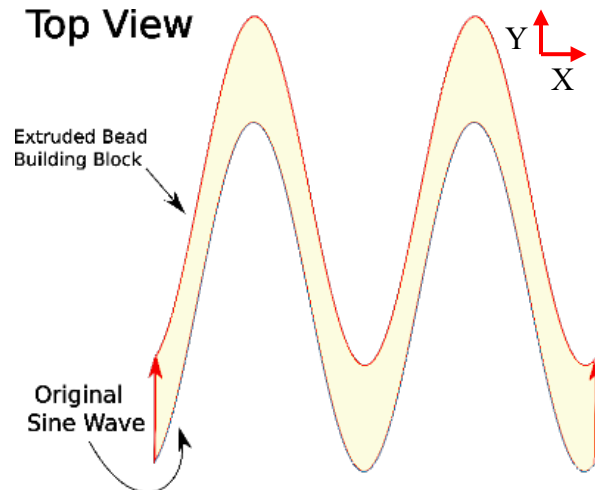


Figure 5 Design of the individual sine wave bead (yellow) to be printed in-plane

This sinusoidal 2-D shape, as with any non-straight shape, has the property that the swept area is not constant. The area in-between the two sine waves is discretized with black normal line segments along a blue midline in Figure 6. Around and at the peaks and troughs of the sine wave, the discretized area (area A2) is larger than in other regions of the sine wave (area A1). This implies that, in order to fill space with an FFF extrusion along the blue midline, the extruded bead width must vary depending on its location along the sine wave. To achieve this, a variable bead width and the CONVEX FFF method (Moetazedian et al., 2021) are used, resulting in the E-Axis commands (incremental filament displacements into the extruder) shown in Figure 6. The extruded bead width is continuously varied along the length of the sine waveform to achieve correct tessellation with the neighboring beads (along the Y axis).

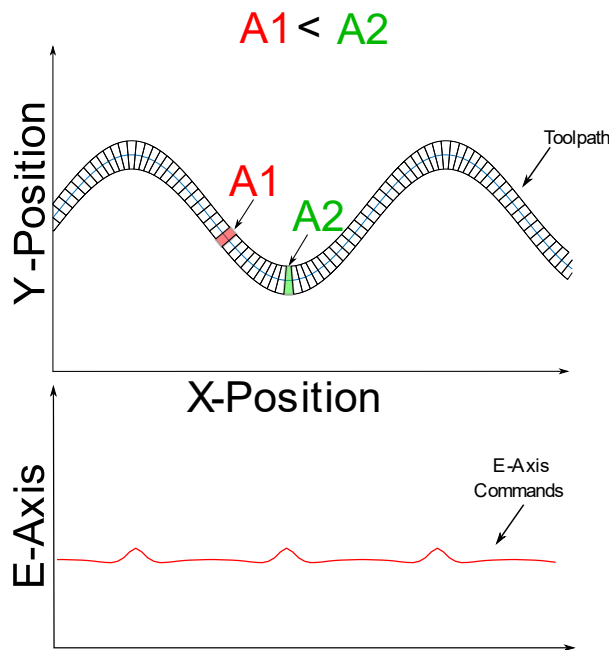


Figure 6 Use of CONVEX for producing accurate sine waveform beads

To generate the G-Code necessary for printing of the pattern, a script was written that uses the area of the discretized elements of the sine wave (see areas A1 and A2 of Figure 6), to generate extrusion values and X-Y-Z trajectory data. The script workflow is shown in Figure 7. These values are then arranged in the standard G-Code format and used to print 150 mm x 150 mm single-layer sheets using a desktop FFF machine, a Prusa Mini (Prusa Research, Prague, Czech Republic).

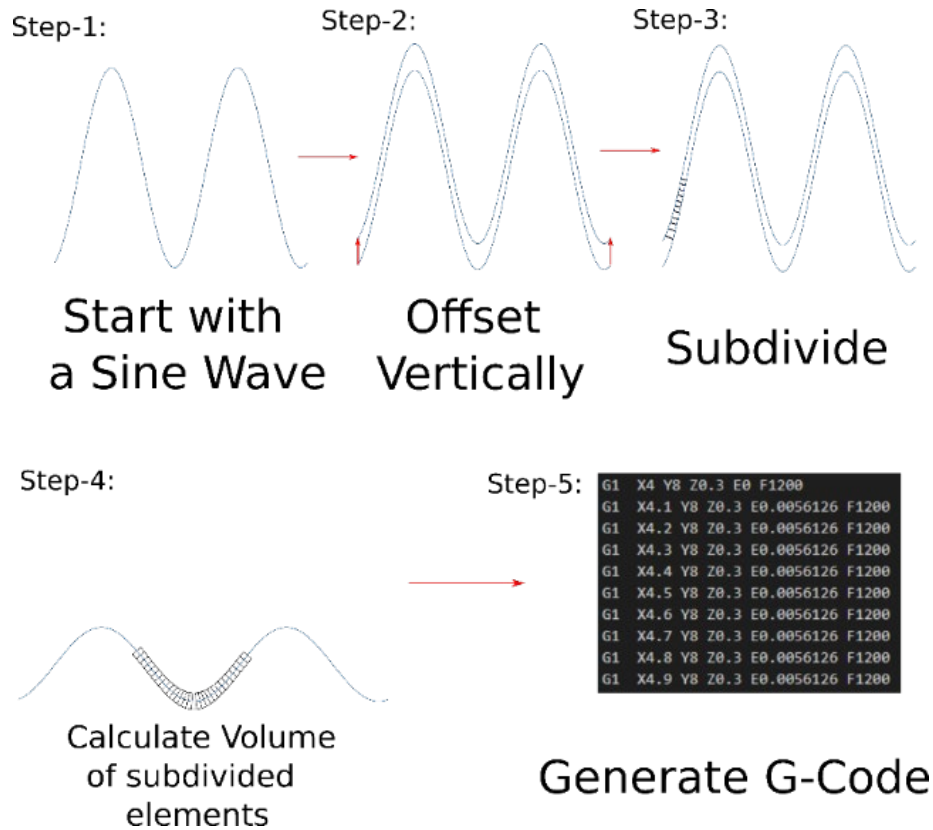


Figure 7 Algorithm workflow for generating G-Code commands

As covered in the Background section, FFF tensile testing samples must be uniformly extracted from a sheet, away from the edges to minimize edge effects such as edge localized stress concentrations at voids. For sample production, we follow the method of Cole et al. (2020) with a slight variation in the method of test sample extraction from the printed sheet. In this work, the samples are extracted using a specimen cutter with a gauge length of 30 mm and a gauge width of 5 mm, following ISO 527-2–Type 1BA (Plastics — Determination of tensile properties). Once the samples are cut, their weight is measured. Tensile testing was done on an Instron 5967 universal testing machine (Instron, Norwood, Mass.) at a strain rate of 10 mm/min, using the 0°, 45°, and 90° orientations shown in Figure 8A. The tests were conducted on 3 to 5 samples for each of the nine test conditions. The steps for this procedure are shown in Figure 8B.

Three sources of G-Code are tested: 1) straight line beads sliced in PrusaSlicer (Prusa Research, 2021) to serve as a control for standard FFF desktop printing, 2) straight line beads

sliced in a custom MATLAB script to serve as a low-speed control, and 3) sine wave beads sliced in a MATLAB script to test the premise of the paper. The sine wave has a period of 5 mm and a peak-to-peak amplitude of 2 mm. The trajectory speed for the MATLAB-script-sliced G-Code is fixed at 250 mm/min (4.2 mm/s) and the layer height is fixed at 0.3 mm. The sine wave period of 5 mm corresponds to a cycle period of 1.2 seconds and a cycle frequency of 0.833 Hz at this speed. The print speed set in the PrusaSlicer-sliced G-Code is 1200 mm/min, which is nearly 5 times that of the MATLAB script. The slow printing speeds of the sine wave beads are required for the sine wave beads due to the use of CONVEX, but for an equal comparison, the same slow speeds are used to print the straight line beads that are sliced in the MATLAB script. The nine test conditions are formed by testing the three orientations (0°, 45°, and 90°) with each of the three slicing methods (straight lines in PrusaSlicer at 1200 mm/min, straight lines in MATAALB at 250 mm/min, and sine wave beads in MATLAB at 250 mm/min).

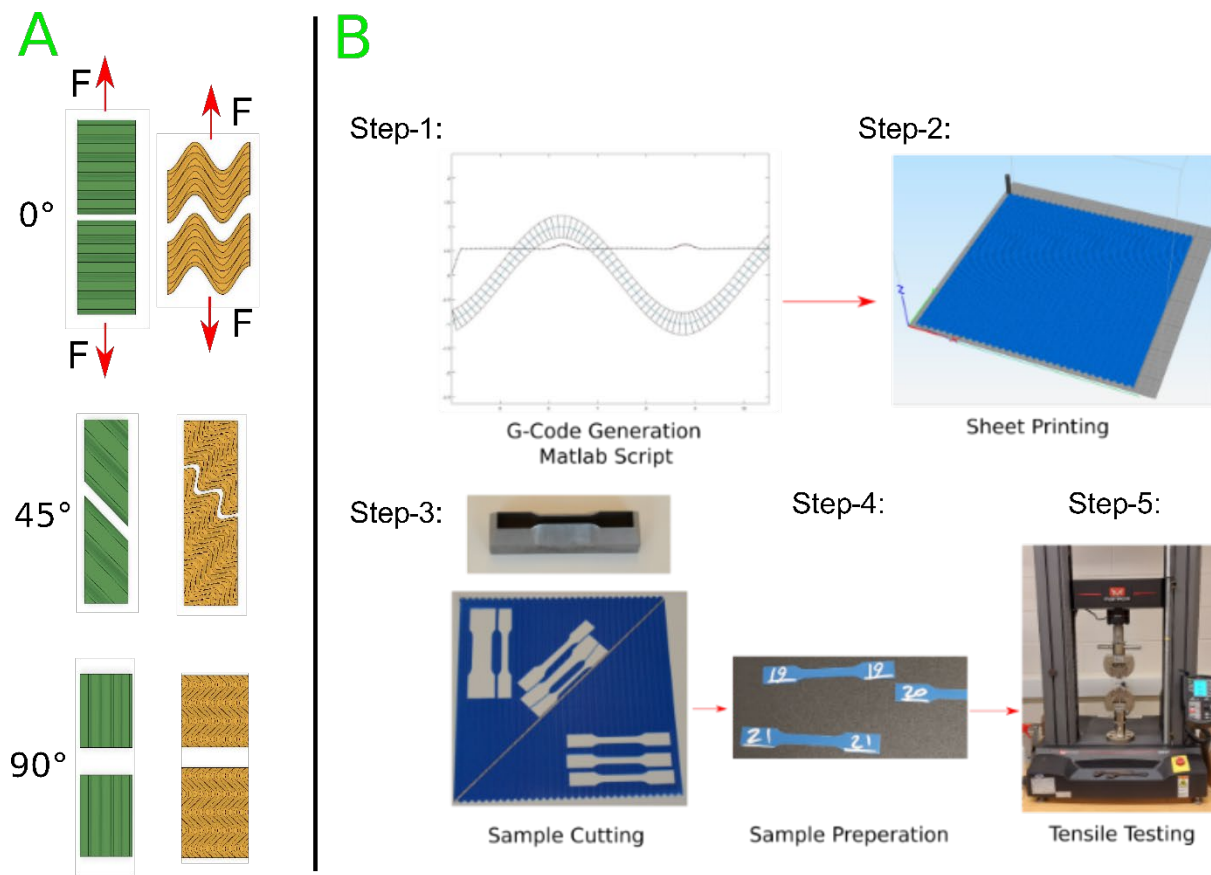


Figure 8 (A) Loading direction, (B) Workflow for generating and testing of specimens

Polymaker PolyMax PLA filament (Polymaker, Shanghai, China) was used in printing of all the sample sheets. The filament color was blue. The filament diameter was 1.75 mm. The filament batch number was 200412802. Printing was conducted with a bed temperature of 60 °C, extruder temperature of 210 °C (this was a first-layer print, so there was no subsequent layer extrusion temperature). The part cooling fan was turned off. The room temperature was around 23 °C. There was no enclosure used around the printer.

Results

Figure 10A shows the average engineering stress vs strain curves of the different sine wave and straight-line samples sliced by the MATLAB script. The results of the tensile tests show a 48.6% reduction in the ultimate tensile strength (UTS) anisotropy of the sine wave pattern. Additionally, the strength was improved by 43% and 29% for the 0° and 45° orientations, respectively. However, a 4% reduction in UTS was observed at the 90° orientation. The anisotropy is calculated by finding the maximum difference in the UTS values between all the loading orientations (0°, 45°, and 90°), this provides the maximum deviation in UTS values, after which, the percent difference is calculated comparing the straight line and sine wave samples. These values and equations are summarized in Table 1.

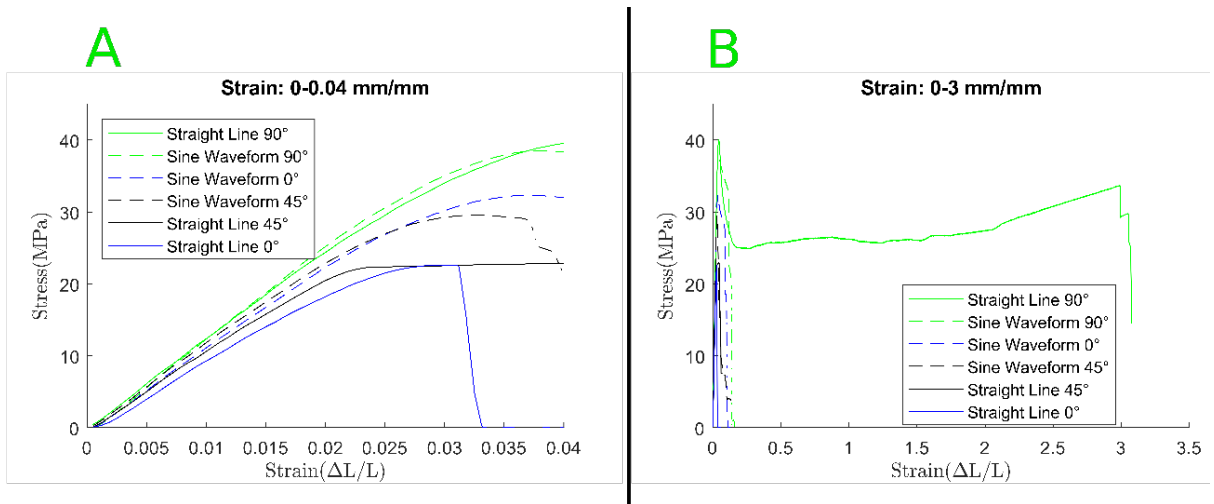


Figure 9 (A) Engineering stress vs. strain with strain values between 0 and 0.04 mm/mm
(B) The complete engineering stress vs. strain curve

Table 1 UTS values and measure of anisotropy in UTS for MATLAB-script-sliced samples only

	Ultimate Tensile Strength (MPa)		
Equation	<i>A</i>	<i>B</i>	$\left(\frac{B - A}{A}\right) \times 100$
Angle	Straight Line	Sine Wave	%Difference
0°	22.59	32.34	43%
45°	22.95	29.54	29%
90°	40.04	38.51	-4%
Equation	MaxDiff(<i>A</i>) = $\max(A(90^\circ) - A(0^\circ) , A(90^\circ) - A(45^\circ) , A(45^\circ) - A(0^\circ))$	MaxDiff(<i>B</i>)	$\left(\frac{\text{MaxDiff}(B) - \text{MaxDiff}(A)}{\text{MaxDiff}(A)}\right) \%$
MaxDiff	17.45	8.97	-48.6%

In a similar manner to the effect on UTS, the toughness was affected by load and extrusion type. Toughness is calculated according to the following equation:

$$\text{Toughness} = \int_0^{\varepsilon_{\text{Final}}} \sigma d\varepsilon$$

Where $\varepsilon_{\text{Final}}$ is the strain at failure, and σ is the engineering stress. For the 0° orientation, the sine wave pattern provides a 1043% increase in toughness over the straight-line extrusions. Likewise, for the 45° orientation, the sine wave pattern provides a 300% increase in toughness. In the 90° orientation however, the sine wave pattern exhibits a 99.6% reduction in toughness, as shown in Figure 10B. Because of the severe loss of toughness to the tough orientation, the sine wave pattern provides a 99.8% reduction in anisotropy of toughness. The values are summarized in Table 2.

Table 2 Toughness values and measure of anisotropy in toughness for the MATLAB-sliced samples

Equation	Toughness (MPa)		Comparison
	A	B	$\left(\frac{B - A}{A}\right) \times 100$
Angle	Straight Line	Sine Wave	%Difference
0°	2.7×10^1	3.1×10^2	1043 %
45°	7.3×10^1	2.9×10^2	300 %
90°	2.0×10^5	6.1×10^2	-99.6 %
Equation	MaxDiff(A) = $\max(A(90^\circ) - A(0^\circ) , A(90^\circ) - A(45^\circ) , A(45^\circ) - A(0^\circ))$	MaxDiff(B)	$\left(\frac{\text{MaxDiff(B)} - \text{MaxDiff(A)}}{\text{MaxDiff(A)}}\right) \%$
MaxDiff	2.0×10^5	3.2×10^2	-99.8%

An interesting failure behavior was observed at the 45° sine waveform pattern, where the failure occurred as a “stepped” process. Instead of a clean fracture, due to the geometry, the fracture initiated at the 0° region of the sine wave, then, the failure propagates with a higher strain-to-failure value to the 90° region. As shown in Figure 13.

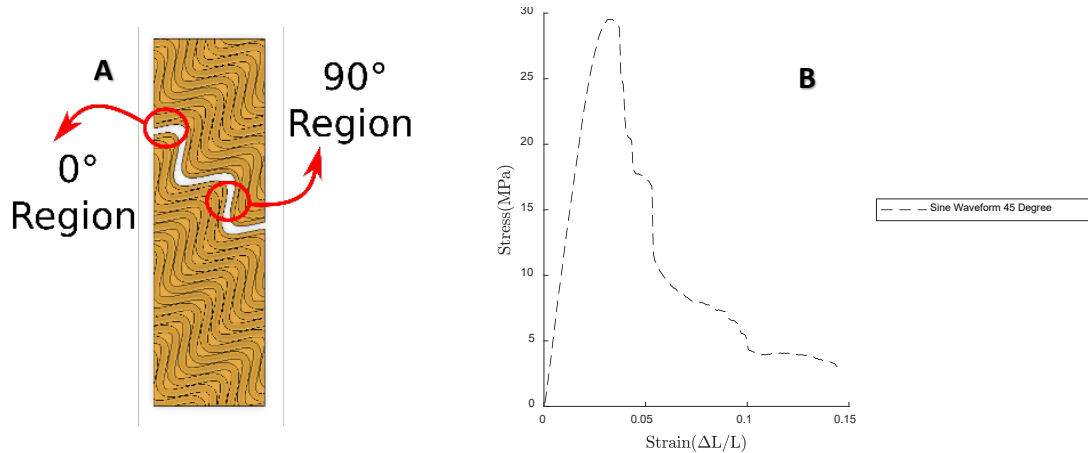


Figure 10 (A) 0° and 90° regions (B) stress vs strain curve showing “Stepped” failure behavior in the 45-degree sine waveform pattern



Figure 11 sine waveform specimen showing "stepped" failure behavior.

To verify that our results are accurate for the straight-line extrusions, we compare our results to the results in Yao et al. (2019). The comparison shows that the G-Code provided by PrusaSlicer provided the closest results, as shown in Figure 15. However, as the G-Code provided by the script is the most similar comparison between the sine wave pattern and straight-line pattern, we select it's results in our analysis (Results summarized in Figure 16).

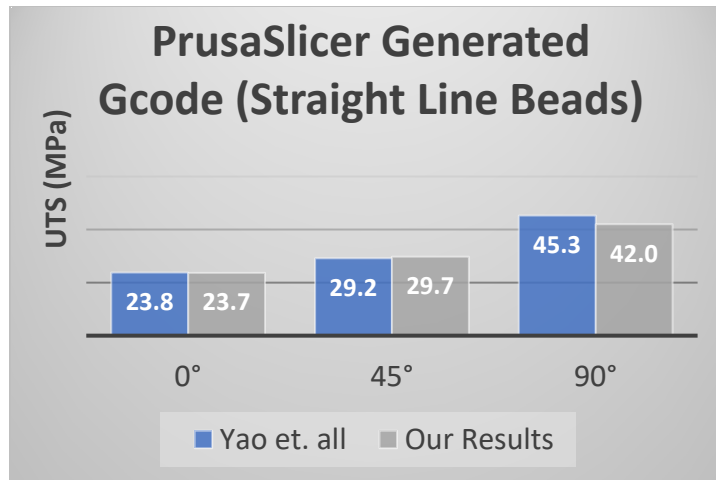


Figure 12 PrusaSlicer provided G-Code UTS values vs. Yao et al. (2019)

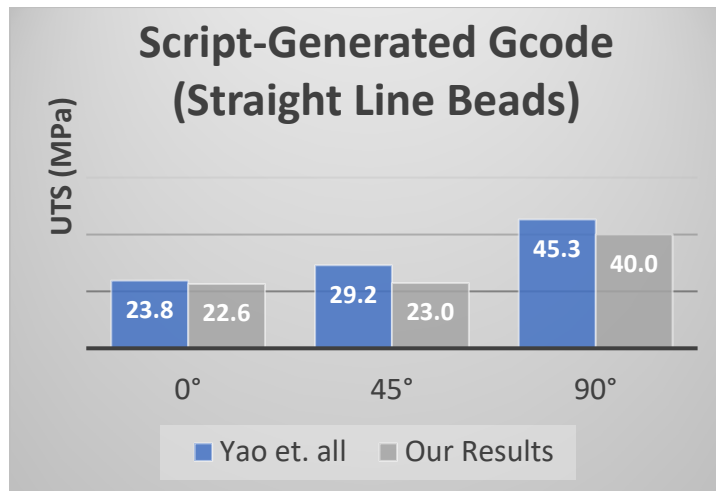


Figure 13 Script provided G-Code UTS values vs. Yao et al. (2019)

To ensure that the increase in strength was not due to a larger mass or thickness, each sample was weighed, the results shown in Table 3 show a small variation of 2% to 4% between the straight-line pattern and sine wave pattern. This difference is much smaller than the

difference in magnitude of strength values. Therefore, we can conclude that the difference in strength is not due to differences in sample weight.

Table 3 Weight values of all MATLAB-script-sliced samples

	Weight (mg)		
	Straight Line 0°	Straight Line 45°	Straight Line 90°
	207	200	198
	207	201	201
	205	201	200
Average	206.3	200.7	199.7
	Wavy Line 0°	Wavy Line 45°	Wavy Line 90°
	200	206	200
	201	203	201
	195	206	200
Average	198.7	205.0	200.3
%Difference	-4%	2%	0%

Conclusion

In conclusion, this study examined strength and toughness and anisotropy of the two in features that are commonly called “horizontal perimeters” as they have 100% infill in-plane. In the results, sine wave beads with continuously varied extrusion width provided higher ultimate tensile strength values under the 0° and 45° loading orientations and a more isotropic behavior than a straight-line bead under identical loading conditions. A benefit of a reduced anisotropy of tensile strength makes it easier to design FFF parts without a priori knowledge of the loading or printing orientations. Furthermore, the minimum UTS in two of the three orientations (0° and 45°) has increased using the sine wave pattern allowing for material savings when orientations are not known. On the other hand, the maximum UTS decreased by 4% in the 90° orientation. while toughness is increased in the 0° and 45° orientations, it is drastically reduced in the 90° orientation. However, PLA is rarely utilized for its toughness, as evident by the variety of modified PLA filaments on the market that claim increased toughness. Therefore, the concern on the loss of toughness is less severe in the case of PLA. In the present paper, the toughness for the straight line beads was measured in three orientations only with 45° increments. As the 90° orientation provides a superior toughness value, while the 0° and 45° orientations provide vastly reduced toughness, the sensitivity of the pattern to the loading orientation is unknown.

Future work is set to tackle the speed disadvantage that is a necessity for accurate sine wave extrusions. This will be partly improved by better modeling and control of the extrusion system. Additionally, the sine wave pattern is to be extended to 3D from the current planar 2D sheets, such that the overall anisotropy of 3D printed objects is reduced, especially between layers. One possible application is the printing of shafts with superior bending strength to that of shafts printed with planar layers.

Appendix A

Supplementary data associated with this article can be found at

<https://www.dropbox.com/sh/op1qmsxes2fh0cu/AABEo2EssWMvk04VXI2ECaFXa?dl=0>

These data include the G-Codes and MATLAB script that was used to generate G-Codes.

References

Cole, D., Gardea, F., Henry, T., Seppala, J., Garboczi, E., & Migler, K. et al. (2020). AMB2018-03: Benchmark Physical Property Measurements for Material Extrusion Additive Manufacturing of Polycarbonate. *Integrating Materials and Manufacturing Innovation*, 9(4), 358-375. doi: 10.1007/s40192-020-00188-y

International Organization for Standardization. (2017). ISO 527-2: Tensile Testing for Plastics.

Khurana, J. B., Dinda, S., and Simpson, T. W. (2017). Active-z printing: A new approach to increasing 3D printed part strength. *Solid Freeform Fabrication Symposium*.

Moetazedian, A., Budisuharto, A., Silberschmidt, V., & Gleadall, A. (2021). CONVEX (CONTinuously Varied EXtrusion): A new scale of design for additive manufacturing. *Additive Manufacturing*, 37, 101576. doi: 10.1016/j.addma.2020.101576

Popescu, D., Zapciu, A., Amza, C., Baci, F., & Marinescu, R. (2018). FDM process parameters influence over the mechanical properties of polymer specimens: A review. *Polymer Testing*, 69, 157-166. doi: 10.1016/j.polymertesting.2018.05.020

Prusa Research (2021). PrusaSlicer (Version 2.3.3) [computer software].
https://help.prusa3d.com/en/article/install-prusaslicer_1903

Singh, S., Singh, G., Prakash, C., & Ramakrishna, S. (2020). Current status and future directions of fused filament fabrication. *Journal Of Manufacturing Processes*, 55, 288-306. doi: 10.1016/j.jmapro.2020.04.049

Yao, T., Deng, Z., Zhang, K., & Li, S. (2019). A method to predict the ultimate tensile strength of 3D printing polylactic acid (PLA) materials with different printing orientations. *Composites Part B: Engineering*, 163, 393-402. doi: 10.1016/j.compositesb.2019.01.025